Physiologic Network-based Brain-heart Interaction Quantification during Visual Emotional Elicitation

Zhipeng Cai, *Member, IEEE*, Hongxiang Gao, *Member, IEEE*, Min Wu, *Senior Member, IEEE*, Jianqing Li, and Chengyu Liu, *Senior Member, IEEE*

Abstract— In recent years, there has been a surge in interest regarding the intricate physiological interplay between the brain and the heart, particularly during emotional processing. This has led to the development of various signal processing techniques aimed at investigating Brain-Heart Interactions (BHI), reflecting a growing appreciation for their bidirectional communication and influence on each other. Our study contributes to this burgeoning field by adopting a network physiology approach, employing time-delay stability as a quantifiable metric to discern and measure the coupling strength between the brain and the heart, specifically during visual emotional elicitation. We extract and transform features from EEG and ECG signals into a 1 Hz format, facilitating the calculation of BHI coupling strength through stability analysis on their maximal cross-correlation. Notably, our investigation sheds light on the critical role played by low-frequency components in EEG, particularly in the δ, θ, and α bands, as essential mediators of information transmission during the complex processing of emotion-related stimuli by the brain. Furthermore, our analysis highlights the pivotal involvement of frontal pole regions, emphasizing the significance of δ-θ coupling in mediating emotional responses. Additionally, we observe significant arousal-dependent changes in the θ frequency band across different emotional states, particularly evident in the prefrontal cortex. By offering novel insights into the synchronized dynamics of cortical and heartbeat activities during emotional elicitation, our research enriches the expanding knowledge base in the field of neurophysiology and emotion research.

Index Terms— Brain-Heart Interaction, EEG Oscillations, Emotion Elicitation, Network Physiology, Time Delay Stability

I. INTRODUCTION

Zhipeng Cai, Hongxiang Gao, Jianqing Li and Chengyu Liu are with the State Key Laboratory of Digital Medical Engineering, School of Instrument Science and Engineering, Southeast University, Nanjing 210096, China (e-mail: zhipeng@seu.edu.cn; hx_gao@seu.edu.cn; ljq@seu.edu.cn; chengyu@seu.edu.cn)

Min Wu is with the Institute for Infocomm Research, A*STAR, Singapore, 138632, Singapore. (e-mail: wumin@i2r.a-star.edu.sg)

EMOTION is a reflection of human subjective feelings and emotional experiences, typically triggered by external stimuli. Emotions are pivotal in daily life, influencing our learning efficiency, decision-making processes, social relationships, and overall happiness. However, our understanding of emotions still needs further depth to effectively manage and regulate emotions, ultimately enhancing our quality of life and psychological well-being.

The human brain's neural networks are crucial for processing emotions, with the amygdala evaluating stimuli's emotional significance and the insular cortex regulating emotions. Electroencephalography (EEG) helps explore emotional processing through different frequency bands and brain regions [1]–[3]. Studies have reported hemispheric θ power asymmetry reflects emotional valence [4], and distraction doesn't affect θ power initially but reduces later activity [5]. Moderate exercise improves negative emotions, reflected in β power changes [6]. In addition, variability in frontal and parietal EEG activity, including α, β, θ/β, and σ/β ratios, relates to individual differences in emotion regulation [7]. Moreover, EEG γ band activity correlates closely with emotional status [8], higher in generalized anxiety disorder patients during worry [9]. Positive emotions activate β and γ bands in the lateral temporal region, neutral emotions elicit higher α in parietal and occipital areas, while negative emotions show elevated δ in parietal and occipital regions and increased γ in prefrontal regions [10].

Emotional changes impact the autonomic nervous system, influencing heart rhythm and ECG features as indicators of emotional status [11]. Heart rate fluctuations correlate positively with empathy, particularly in individuals with consistent response patterns [12]. Heart rate variability (HRV) can reflect emotional responses: high-frequency oscillations are vagally regulated, while low-frequency involve both vagal and sympathetic activities [13]. Maternal emotional status during pregnancy influences fetal HRV, suggesting effects on fetal nervous system development [14]. Furthermore, elevated HRV enhances emotional well-being, likely due to high-amplitude oscillations impacting brain network dynamics [15]. Heart rate responses differ across emotions: fear induces pronounced heart rate fluctuations, sadness increases signal complexity, and happiness alters sympathetic-parasympathetic balance [16].

Over the past decade, scholarly interest has surged in

exploring the dynamic interactions between the central nervous system and the peripheral cardiovascular system. The brain's autonomic nervous system, including the amygdala and insular cortex, regulates heartbeat rhythm during emotional processing [17]. Conversely, cardiac afferent input shapes brain functions related to perception, cognition, and emotions, involving regions like the amygdala and hypothalamus [18]. Insular cortex damage post-stroke can lead to cardiovascular instability and autonomic nervous system alterations [19]. Moreover, psychological stress impacts the prefrontal cortex, contributing to severe arrhythmias [20]. Unpleasant music reduces heart rate with increased frontal midline θ power [21]. Negative emotions correlate EEG θ activity with the right prefrontal cortex, aligning with sympathetic response [22]. Meditation shows a positive correlation between HRV high-frequency power and EEG frontal midline θ power [23]. band power correlates with HRV complexity during relaxation, while β band power links with HRV powers during affective picture viewing and physical stress [13], [24]. While existing studies have probed the impact of emotions and emotional responses on the brain-heart connection, a comprehensive understanding of emotions' neural mechanisms necessitates further exploration of brain regions and their interconnections.

The quantification of functional BHI presents methodological challenges due to its intrinsic multimodal and multivariate nature, diffuse distribution over the central nervous system, and directionality issues. Additionally, the non-stationarity, nonlinearity, complexity, and multi-scaling of BHI need to be considered when applying classical signal processing tools. To date, various techniques have been developed to measure or model these interactions, such as correlation coefficients, maximum information coefficients (MIC), phase-locking values (PLV) or phase lags indexes (PLI), Granger Causality (GC), transfer entropy (TE) and time-delay stability (TDS) [13], [25]. The Pearson correlation coefficient is an undirected measure to describe the degree of association between two continuous variables. It has been used extensively in studies exploring the heart-brain coupling relationship, because of its simplicity of calculation and ease of manipulation [26]. MIC can measure both linear and nonlinear coupling between two dynamical systems based on the calculation of mutual information [13]. As another undirected measure, TDS is a network-based approach used to study the dynamics of multiple interconnected systems as they transition from one physiological status to another [27]. GC is a directed measure for determining whether one signal can be used to predict the value of another signal, with the statistical assumption that the data has a normal distribution with uniform variance, but it is less efficient in detecting specific nonlinear causal relationships [28]. TE is a non-parametric measure of how information is transferred between two signals. It is particularly useful when evaluating nonlinear couplings without the need for a priori information [29]. CCM is a time-invariant method to quantify directional nonlinear interactions between dynamical systems, and has been successfully exploited to characterize temporal lobe epilepsy [30] and schizophrenia [25]. Despite comprehensive descriptions of psychophysiological changes from both single-system and cross-

system perspectives, the mechanisms governing transitions between emotional status and their impact on the strength of physiological interactions and the topology of physiological networks are still under investigation.

In this paper, a network-based strategy involving TDS was adopted to measure the coupling strength among physiological systems, and the alterations in physiologic network topology were investigated to signify transitions between different emotional statuses. The interactions among brain rhythms across and within cortical locations were investigated. In addition, the dynamic interactions between the brain and heart during emotion elicitation were quantified. Furthermore, we tested the statistical significance of the results using various surrogates that build on different null hypotheses.

II. METHOD

A. Data

The DEAP database is a multi-modal database designed for studying human emotions. It includes physiological signals collected from 32 participants (50% male, 50% female) with an average age of 26.9 years. The experiment started with a 2-minute base recording, then participants watched 40 different 1-minute videos, with each video eliciting emotions recorded through 32-channel EEG and 8-channel peripheral physiological signals. The data were segmented into 63-second intervals, with the first 3 seconds serving as a pre-trial base. In this study, to prevent data contamination by varying emotional status, particularly with longer video stimuli, only the physiological recordings from the final 60 seconds of each film clip were selected for subsequent analysis.

The 32-channel EEG were recorded using a Biosemi ActiveTwo system according to the international 10-20 system, along with 8-channel peripheral physiological signals: 2 ophthalmic signals, 1 skin electrical signal, 2 EMG signals, 1 respiratory record, 1 plethysmography, and 1 temperature record. All the signals were measured at 512 Hz sampling frequency. In this study, only 14 EEG channels (AF3, F7, F3, FC5, T7, P7, O1, O2, P8, T8, FC6, F4, F8 and AF4) were used, and all the signals were resampled to 1 kHz to ensure the accuracy of HRV calculations. The decision to exclude 18 channels and focus on 14 electrodes was based on prior studies [31], [32], which emphasized the importance of selecting specific channels relevant to emotional activity to improve classification accuracy. Practical considerations, including equipment limitations and the use of devices like the Emotive Epoc headset with its 14 channels, also influenced this choice. After each experiment, participants were instructed to rate their emotional experiences using the Self-Assessment Manikin (SAM) scale, providing arousal, valence, liking, and dominance ratings on a scale of 1-9.

This study focuses on examining the dynamic interactions between the brain and heart in response to emotion elicitation, particularly emphasizing the arousal dimension. Emotional status is classified as high arousal (HA) and low arousal (LA), with the status preceding elicitation (Base) considered for comparative analysis. Distinctions are made based on participants' subjective ratings, with a threshold set at 5.
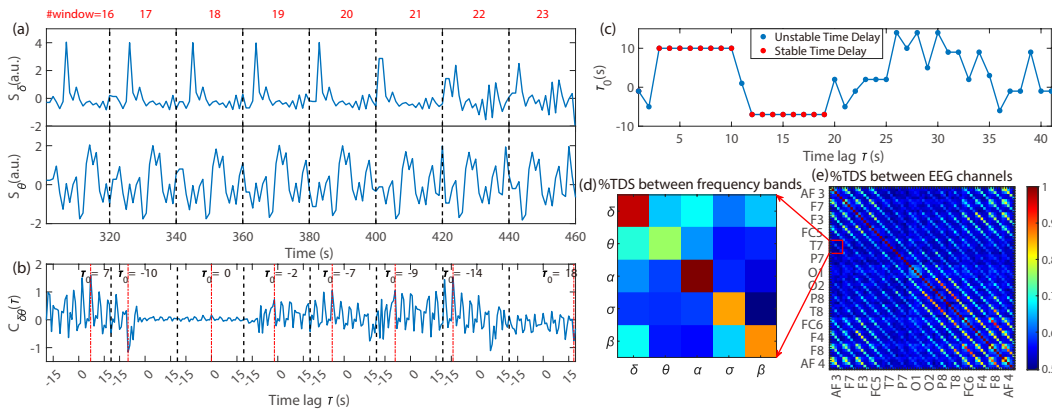
Fig. 1. Schematic of TDS method and its application in brain rhythms coupling strength representation. (a) Sequential segments of EEG spectral power (S_δ and S_θ) of the δ and θ band shown for consecutive 20 s windows. (b) Cross-correlation ($C_{\delta\theta}$) of S_δ and S_θ within each window across the lags between two signals, and the time lag τ_0 corresponding to the maximum represents the time delay. (c) Time delay τ_0 between S_δ and S_θ for consecutive 20 s windows moving with 1 s overlapping. (d) %TDS matrix representing the coupling strength between T7 channel and AF3 channel at different physiologically relevant EEG frequency bands ($\delta, \theta, \alpha, \sigma, \beta$). (e) %TDS block-matrix representing the average coupling of all brain rhythms across each pair of EEG channels (AF3, F7, F3, FC5, T7, P7, O1, O2, P8, T8, FC6, F4, F8, AF4). Each block along the diagonal corresponds to the coupling within different frequency bands of the same EEG channel, while each off-diagonal block represents the coupling between specific pairs of EEG channels.

B. Physiologic Network Interactions

1) Featured Waveform Extraction: The purpose of this paper is to study the brain-heart coupling in different emotional statuses, 14-channel EEG and lead-II ECG signals from the DEAP database were used in this study. To compare these very different signals with each other and to study the interrelations between them, all time series are converted to the same time resolution of 1 s before the analysis.

For EEG signals, the independent component analysis (ICA) of the EEGLB toolbox is used. Preprocessing was performed in EEGLAB, and EEG signals were high-pass filtered at 1 Hz using the ***pop_eegfiltnew*** function. Next, bad channels are identified and removed with the ***pop_select*** function based on visual inspection. After preprocessing, the ***pop_runica*** function, using the default ***infomax*** algorithm with the recommended 'extended' option enabled, is employed to perform ICA on the EEG data. ICA decomposes the EEG signals into independent components, some of which represent noise or artifacts such as eye blinks, muscle activity, or electrical interference. These components are then inspected visually using the ***pop_selectcomps*** function, allowing for the identification of noise-related components. Once identified, these components are removed from the data using the ***pop_subcomp*** function. Finally, the cleaned EEG data is used for following process. Subsequently, the Hanning window is applied, and the sliding window method is employed to segment the signal into multiple time windows, each of which is L in duration with s window shift. Within each time window, the Short-Time Fourier Transform is utilized to convert the time-domain signal into the frequency-domain signal, thereby capturing the frequency components of the signal within the current time window. Let $x(t)$ be the EEG signal in the time domain, the frequency components of the signal within the current time window at f frequency band $\mathbf{P}(f,t)$ is

$$\mathbf{P}(f,t) = \int_{-\infty}^{\infty} x(\tau,s) \cdot \omega(\tau-t) \cdot e^{-j2\pi f\tau} \, d\tau \qquad (1)$$

where $\omega(t)$ is the Hanning window function, and s represents the window shift.

Finally, similar as in [27], the spectral power $\mathbf{S}(f)$ of five frequency bands (δ waves (0.5 – 3.5 Hz), θ waves (4 – 7.5 Hz), α waves (8 – 11.5 Hz), σ waves (12 – 15.5 Hz) and β waves (16 – 19.5 Hz)) is computed by squaring the magnitude of the signal in the frequency domain.

$$\mathbf{S}(f,t) = |\mathbf{P}(f,t)|^2 \qquad (2)$$

For the ECG signal $y(t)$, the QRS locations of each heartbeat are detected using an R peak detector, which employs stationary wavelet transforms for real-time beat detection from single-lead ECG signals with the Daubechies 3 ('db3') wavelet as the mother wavelet [33]. Following this peak detection, the RR interval sequence is derived by computing the time intervals between successive QRS peaks. Subsequently, the heart rate, expressed in beats per minute, is calculated. To ensure compatibility and standardization, the heart rate values are inverted, and resampling is applied to transform the heart rate into a discrete 1 Hz (1 s bins) format for further analysis and interpretation.

2) BHI Coupling Strength Calculation: To investigate the interaction between two physiological systems $\mathcal{X}$ and $\mathcal{Y}$, their respective output featured waveforms $\mathbf{X}$ and $\mathbf{Y}$ are partitioned as $\mathbf{X} = \{\mathbf{X}^i\}_{i=1}^{N_L-1} \in \mathbb{R}^{N_L \times L}$ and $\mathbf{Y} = \{\mathbf{Y}^i\}_{i=1}^{N_L-1} \in \mathbb{R}^{N_L \times L}$ with a window shift of s, where $N_L = |\mathbf{X}| = |\mathbf{Y}|$ denotes the number of segments and L denotes the time span of each segment, as shown in Fig. 1 (a). To get enough R-waves in the ECG, these segments have an equal length of $L = 20$ s, with a window shift of s. Consequently, the $N_L = (N - L)/s + 1$, where N is the length of featured waveforms. Thereafter, the segmented featured waveforms undergo individual normalization to attain zero mean and unit standard deviation. This procedure eliminates constant data trends, renders the signals dimensionless, and ensures that the estimated coupling between featured waveforms $\mathbf{X}$ and $\mathbf{Y}$ remains uninfluenced by their relative amplitudes.

Then, the cross-correlation function between two physiological systems is calculated as $C_{\mathcal{X}\mathcal{Y}}$ by applying periodic boundary conditions, where τ is the lag. For each segment i, the position corresponds to the maximum in the absolute value of $C_{\mathcal{X}\mathcal{Y}}^i(\tau)$ is defined as the time delay τ_0^i (Fig. 1 (b)).

$$C_{\mathcal{X}\mathcal{Y}}^i(\tau) = \frac{1}{L}\sum_{l=1}^{L}\mathbf{X}_{l+(i-1)\cdot s}^i \cdot \mathbf{Y}_{l+(i-1)\cdot s+\tau}^i \quad (3)$$

$$\tau_0^i = \operatorname{argmax}_\tau \ |C_{\mathcal{X}\mathcal{Y}}^i(\tau)| \quad (4)$$

Two physiological systems are identified as linked if considered interconnected when their corresponding featured waveforms display a consistent time delay that does not change by more than ±1 s across multiple consecutive time windows. According to [27], for each τ_0 in time series τ_0^i, the segments are considered as stable when for at least $0.8*H$ out of H consecutive segments the time delay remains in the interval $[\tau_0\text{-}1, \tau_0\text{+}1]$. Mathematically, this can be expressed as:

$$Stability(\tau_0) = \sum_{i=1}^{N-L+1}\mathbb{I}(|\tau_0^i - \tau_0| \leq 1) \geq 4 \quad (5)$$

where $\mathbb{I}(\cdot)$ is the indicator function.

The process of identifying intervals with stable time delays is iterated using a sliding time window with a step size of one along the entire series τ_0^i.

Subsequently, the coupling strength of two physiological systems is determined as the fraction (%TDS) of stable points in the time series τ_0^i, as shown in Fig. 1 (d)-(e). Thus, longer periods of TDS between two systems' featured waveforms indicate more stable interaction and stronger coupling, with link strength in physiological networks determined by %TDS.

$$\%\text{TDS} = \frac{Number\ of\ Stable\ Points}{N-L+1} \quad (6)$$

III. EXPERIMENTS AND RESULTS

A. Parameters Selection for Physiologic Network Construction

1) Window Shift for Signal Segmentation: In the process of physiologic network construction, window shift s is an important parameter. It affects the degree of overlap between consecutive windows $(N-s)$ and the final number of windows $(N_L = (N-L)/s + 1)$ obtained. To assess the influence of s on BHI, we compared the effects of different s values ranging from 1 to 9 with a step size of 1 on the average link strength (ALS) (Fig. 2 (a)). The number of consecutive windows H is set to 5. The ALS, measured in %TDS, represents the mean of all elements in the TDS matrix for each emotional status. It reflects the average strength of all links in a network across subjects and film clips. This comprehensive analysis provides insights into the evolving dynamics of brain rhythm interactions in response to varying emotional status. It can be seen that the average strength of network links exhibit variations with transitions in emotional status, with the Base displaying significantly stronger network links compared to HA and LA. In addition, the ALS of constructed physiologic network increases with s grows among all three emotional
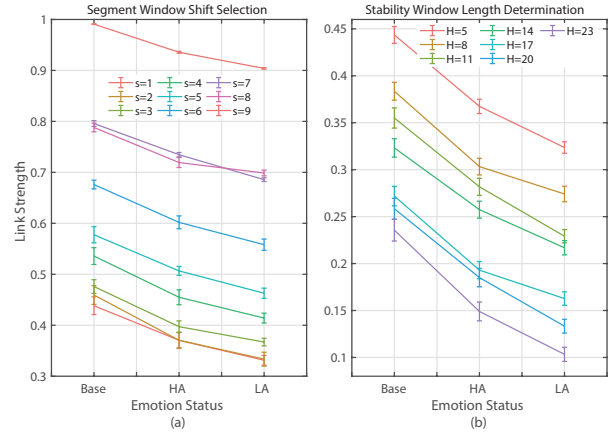

Fig. 2. Parameters selection for physiologic network construction. (a) Comparison of different s on average link strength, (b) the effect of consecutive windows numbers H on stability determination.

statuses (expect s=7 and s=8 in LA). When the s reached 9, the ALS is almost 1 in Base status, with ALS > 0.9 in the other two statuses. It means that all the EEGs among brain rhythms across cortical areas are coupled with the heart. Considering the consistent trend of ALS across different s values and the requirement for an adequate number of H for stability calculations, we selected s=1 for our subsequent experiments.

2) Window Length for Stability Determination: The stability of two physiological systems is related to the number of consecutive segments H in the time delay. Therefore, we evaluated the effects of different H ranging from 5 to 23 with a step of 3 on ALS (Fig. 2 (b)). The consequent stable segments $(0.8*H)$ for each H are 4, 6, 9, 11, 14, 16, and 19, respectively. Similar to the influence of s on ALS among three emotional statuses, the ALS presents a descending trend from Base to LA. Conversely, regardless of the emotional status, the ALS decreases with the increase of H. It indicates that with a larger H and a fixed stability ratio (0.8), it is difficult to maintain stability between two systems, resulting in lower ALS. To improve computational efficiency and ensure sufficient link strength, we chose H=5 as the parameter for our subsequent analysis.

B. Brain-Brain Networks

1) Inter-channel Brain Interactions: To gain a comprehensive understanding of the influence of same-frequency interactions across brain areas and their responsiveness to changes in emotional status, we present chord diagram representations of frequency-specific networks in Fig. 3 (a). These diagrams depict the ensemble of inter-channel links connecting a specific frequency band at different brain locations (network nodes). Our findings reveal that brain interactions mediated by specific frequency bands in a given physiological status exhibit distinct network structures and patterns during transitions between emotional status. Comparison of specific frequency networks under the same physiological status reveals significant variations in network connectivity and link strength across different frequency bands. In the Base status, preceding visual emotional elicitation, nearly all brain rhythms participate in
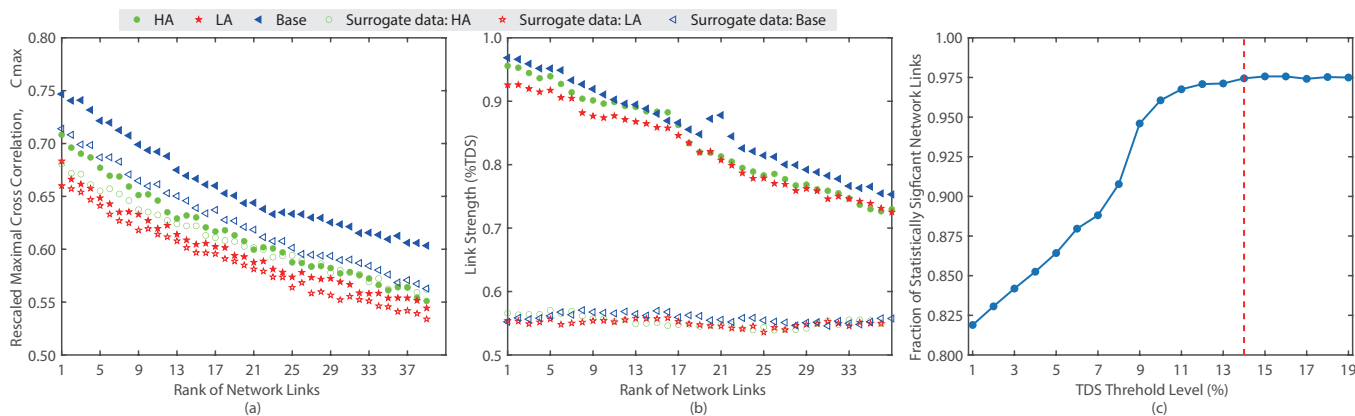
Fig. 3. Brain-Brain interaction among and across brain rhythms. (a) Chord diagram representation of frequency-specific network interactions across brain areas between emotional status. The various colored arcs within the circles represent different EEG channels, and the connections between them indicate their respective coupling strengths. (b) network presentation of the %TDS matrices at 14 cortical locations for different emotional stages (only links with %TDS$\geq$ 0.45 are shown).

mediating inter-channel interactions except for the β band. During HA and LA status, the networks involving δ, θ, and σ bands dominate inter-channel brain wave communications, with higher coupling strengths observed in HA compared to LA. Furthermore, with increasing frequency of brain rhythms, the left and left posterior brain regions gradually diminish in their involvement in inter-channel brain wave communications. This is evident in the near absence of contributions from almost the entire left brain region (AF3, F7, FC5, T7, P7, O1) to inter-channel interactions.

2) Intra-channel Brain Interactions: To better understand the inherent dynamics of brain activity within specific regions, we delved into intra-channel networks, which illustrate the coordination of brain activation across frequency bands within the same location (i.e., the same EEG channel), as shown in Fig. 3 (b). Notably, lower-frequency brain rhythms, such as δ with θ, exhibit stronger coupling, particularly observed in frontal brain areas (AF3, F7, F3, FC5, FC6, F4, F8, AF4). Additionally, the transition between emotional status induces a significant reorganization in both link strength and topology for all local networks of brain rhythm interactions. During the Base status, robust connections within local networks of brain rhythm interactions are observed, with high intra-channel brain network connectivity across all EEG channel locations. However, following visual stimulation, whether in a HA or LA status, link connectivity and connection strength diminish in both central and occipital areas, except the O1 channel. Generally, the local network of brain rhythm interactions in HA exhibits stronger connections than those in LA, especially for the F8 channel.

C. Brain-Heart Networks

1) Surrogate Analysis and Statistical Assessment: A time-shift surrogate analysis was conducted to examine the cross-correlation strength $C_{\max}$ (the global maximum of the cross-correlation function) (see Fig. 4 (a)). To generate "shift surrogate data", one dataset was temporally shifted relative to the other, with surplus values wrapped around to the beginning of the dataset. This method preserves the statistical structure of the original time series while disrupting correlations between them. Three hundred random time shift lags were selected, ensuring that time shifts exceeded 20 seconds. The results indicate that the surrogate test applied to traditional cross-correlation analysis does not reveal any discernible difference between the rank distributions obtained from surrogate and real data. Analysis of the time-shift surrogate data reveals consistent trends: $C_{\max}$ is consistently lower than real data during LA, higher during HA, and highest during Base. However, the surrogate tests do not demonstrate any statistical difference between the surrogate and original rank distributions of $C_{\max}$. These findings suggest that, in this context, cross-correlations do not provide physiologically relevant information regarding the interaction between systems.

To assess the efficacy of the TDS method in capturing physiologically relevant information concerning endogenous interactions between systems, an inter-subject surrogate test was conducted. This involved pairing physiological signals from different subjects to eliminate physiological coupling. As illustrated in Fig. 4 (b), rank distributions corresponding to different emotional statuses demonstrate varying strengths of network links measured in %TDS. Notably, the rank distribution associated with LA shows a pronounced shift towards

Fig. 4. Surrogate analysis for the validation of BHI. (a) Rank distribution of the maximal cross-correlation (Cmax) for time-shift surrogate analysis, (b) rank distribution of the network link strength (%TDS) for inter-subject surrogate analysis, (c) significant threshold level determination for %TDS.

lower values for network link strength, whereas the distribution for Base consistently exhibits higher values for all links compared to HA. The inter-subject surrogate test, employing TDS analysis to eliminate endogenous physiological coupling, yields significantly reduced link strength p-value$<10^{-3}$ and nearly uniform rank distributions across different emotion statuses. This suggests that the TDS method effectively reveals physiologically relevant information.

Additionally, to compare interactions between physiological systems with varying strengths and changes across different physiological states (e.g., transitions across emotional stages), we establish the significance threshold as the percentage of %TDS at which all links in the physiological network are deemed statistically significant. This determination involves comparing the distribution of original %TDS values with that of %TDS values obtained from 300 surrogates. A Student's t-test is then conducted to ascertain the statistical significance between these distributions for each pair of systems (links) in the network. Network links are deemed significant when the t-test p-value is less than 10^{-3}. The significance threshold level for %TDS is consequently defined as the value above which all network links are statistically significant, indicating endogenous interactions between physiological systems. We find that a threshold of approximately 14 %TDS is necessary to identify networks of statistically significant links across all emotional statuses (Fig. 4 (c)).

2) Dynamics of Brain-Heart Interactions: To elucidate the neurophysiological interactions between the brain and heart during visual emotional elicitation, we investigated to identify and quantify the networks of interactions between these systems. The intricate communications and their modulation with emotional status are visually depicted using radar charts (Fig. 5 (a)). The BHI network exhibits a relatively symmetric distribution of ALS across different brain areas, with a slight prevalence in strength observed for links between the heart and temporal brain areas (T7 and T8). A systematic examination of BHI link strength across all five frequency bands and various emotional statuses reveals that the ALS for the entire brain-heart interaction network is highest during the base status, lower during HA, and lowest during LA. This finding suggests that the strength of all links in the brain-heart network, irre-

spective of brain areas or frequency bands, follows a similar modulation pattern during transitions across emotional status.

To illustrate the change patterns of BHI link strengths across EEG channels during different emotional statuses, the averaged %TDS were projected to the scalp (Fig. 5 (b)). The change patterns of BHI link strengths among different emotional statuses exhibit similarities in some EEG channels. In the δ frequency band, the frontal regions present lower BHI coupling, while exhibiting higher link strength at FC6, P7, and F3 channels. In the α band, BHI showed strong coupling in the right frontal lobe but weak coupling in the occipital lobe. Inversely, BHIs at the σ frequency band exhibit significant differences among different emotional statuses, regardless of EEG channels. Moreover, in the β band, BHIs have an obvious bipolar distribution in the central region at HA and Base status. Most obviously, the θ frequency band exhibit significant arousal-dependent changes among different statuses, especially in prefrontal cortex.

Furthermore, the correlations of BHI between brain rhythms and locations under different emotional statuses are quantified by the Kendall rank correlation coefficient. The p-values are listed in Fig. 6. Significant correlations (p-value<0.05) are denoted with green color, and extremely significant correlations (p-value<0.001) are marked with red color. The interactions between the brain and heart show extremely significant correlations among more than half of the EEG channels at the β, θ and δ frequency bands. BHI is less relevant with the α band, as the p-value<0.001 is observed at only three EEG channels. All statistical analyses were conducted using MATLAB (R2023a) on a PC with an Intel® Core™ i7-7700 3.6 GHz processor and 32 GB RAM.

IV. DISCUSSION

A TDS-based method was adopted to identify and quantify the coupling of physiological systems during visual emotional elicitation in this paper. We investigated the interactions among brain rhythms across and within cortical locations (cross-brain-wave interactions at the same locations and same-brain-wave coordination across brain areas), and their relation to neural plasticity in response to changes in autonomic regulation underlying different emotional statuses. We also studied the
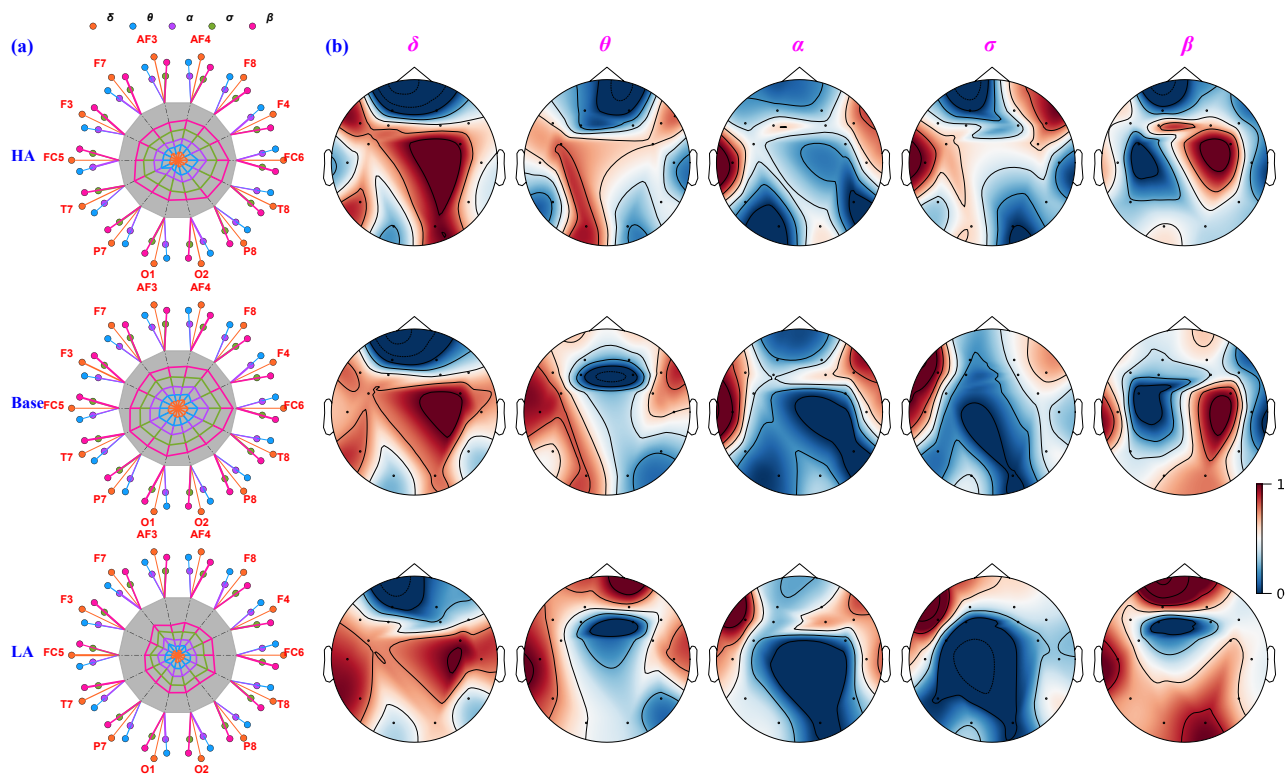
Fig. 5. Brain-heart interactions during different emotional statuses. (a) Network representation of coupling strength between heart and different EEG channels across brain rhythms. Radar charts, centered within hexagons, illustrate the contribution of brain control from distinct brain areas to network link strength across various emotional statuses. Each segment's length along the radius in the radar charts reflects the TDS coupling strength between the heart and each frequency band at respective EEG channel locations. These segments are color-coded to match the corresponding EEG frequency nodes, providing a visual representation of how different brain regions influence network links throughout different emotional statuses. (b) Topographical maps of the averaged BHI in the five canonical frequency bands. For each subfigure, from top to bottom: HA, Base, and LA emotions; from left to right: δ, θ, α, σ, and β bands. For each frequency band, we normalized the averaged BHI to range from 0 to 1 across the three emotional states and four stimulus patterns.
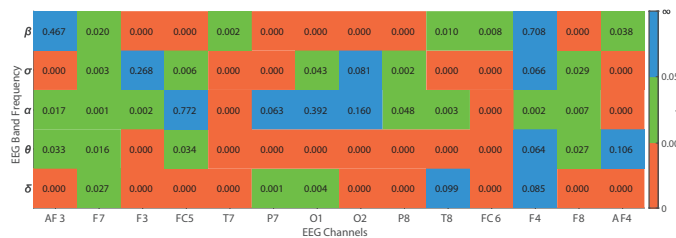
Fig. 6. Kendall rank correlation coefficient for BHI between brain rhythms and locations under different emotional status. Significant correlations (p-value<0.05) are denoted with green color, and extremely significant correlations (p-value<0.001) are marked with red color.

dynamical features of brain-heart networks to establish an association of network structure and dynamics with emotional status and physiologic function.

A. Brain-Brain Networks

The examination of inter-channel brain networks across distinct emotional statuses reveals a notable observation concerning the configuration of the network of brain wave interactions. Particularly, the most substantial transformations occur within the links representing interactions between brain waves of different frequencies (see Fig. 2). This remarkable reorganization in network connectivity and link strength among

diverse brain waves signifies a noteworthy degree of neural plasticity, suggesting the modulation of global cooperative behavior in brain wave interactions to effectively accommodate physiological functions during various status. Consequently, these findings underscore the intricate mechanisms underlying the adaptability of the brain. The analysis of Fig. 5 reveals the presence of denser network linkages within the δ and θ bands. This observation suggests that low-frequency components in the EEG may facilitate information transmission during the brain's focused processing of emotion-related information. Notably, these findings diverge from Lindquist's research, which predominantly associates high-frequency bands with emotion processing, particularly highlighting negative emotional processing [34]. However, our results align with their findings indicating a lack of sensitivity to emotional stimulus variations in low-frequency activity. Additionally, the study conducted by Schubring *et al.* [35] discovered a correlation between high-arousing pictures and spectral power in the α and lower β frequency bands, which correspond to the α, δ, and β bands as examined in our research. Notably, the α band-related brain network connection density was found to be lower in the status of HA compared to both LA status and Base status. This observation is in line with the prevailing notion that α power reflects cortical inhibition or idle status of the cortex, thereby exhibiting an inverse relationship with

cortical activation-–lower α power indicating greater activation [36]. One possible explanation for this observation is that the activity in the medial prefrontal regions of the brain within the β band displayed distinct patterns associated with positive emotions [37].

The network of brain rhythm interactions within 14 cortical regions was meticulously examined to investigate the coordination of brain activation across frequency bands at identical locations. Our inquiry revealed that distinct brain regions exhibit varying degrees of cross-frequency coupling within the same emotional status. Specifically, frontal areas demonstrated highly connected networks, indicative of robust interactions across all frequency bands. In contrast, central areas exhibited lower connectivity, while occipital areas displayed the lowest level of connectivity. This pattern of cross-frequency coupling is attributed to the generation of different brain rhythms by neuronal populations in the 14 cortical layers, subsequently projecting onto the scalp. Consequently, this naturally gives rise to cross-frequency coupling at the same anatomical location, reflecting the synchronous activities of neuronal populations and quantifying the inter-layer coordination among cortical neurons. This result aligns with previous research, suggesting that the frontal cortex is an integration area, facilitating the integration of multi-modal sensory information and emotional reactions, and playing a vital role in social cognition and emotional evaluation [38]. The δ-θ coupling at frontal pole areas exhibited the greatest strength among the 14 cortical regions, a phenomenon substantiated to have significant implications for semantic cognition [39]. Furthermore, the coupling related to the α frequency band displayed variations contingent upon emotional status, providing empirical support for the current understanding of the impact of cognitive and emotional tasks on α-waves [40]. Observations also indicated that the δ-α-σ couplings in most channels manifested divergences across distinct emotional status, suggesting that the cross-frequency coupling of brain oscillations could enhance our comprehension of the neural mechanisms underlying emotions [41].

B. Brain-Heart Networks

To validate the statistical significance of observed data and discern genuine patterns from random fluctuations, surrogate analyses were employed, comparing original data with randomized surrogate data. Based on the results of the time-shift surrogate test (Fig. 4 (a)), it can be inferred that the TDS method exhibits greater reliability in identifying physiological coupling when contrasted with traditional cross-correlation analyses. This conclusion is rooted in the observation that cross-correlation analyses are ill-suited for heterogeneous and non-stationary signals, and are susceptible to the influence of auto-correlations within these signals [27]. Additionally, upon applying the TDS method to inter-subject surrogate data, we observed nearly uniform rank distributions with decreased link strength, as illustrated in Fig. 4 (b). This decline indicates the absence of physiological interactions. Moreover, all surrogate distributions exhibited a consistent pattern, indicating that the stratification of emotion status observed in real data

corresponds to alterations in physiological coupling associated with transitions in emotion status. The rank plots derived from the inter-subject surrogate test further reveal that link strength consistently diminishes during LA, increases during HA, and peaks during Base. This trend may be linked to the gradual augmentation of auto-correlations within the signal output of physiological systems [42].

The analysis of the coupling between 5 brain rhythms from 14 cortical locations and the heart was conducted to elucidate the mechanisms governing the regulation of brain-heart dynamics during emotional arousal. As depicted in Fig. 5 (a), during the HA status, the α band exhibited stronger coupling to the heart, followed by β and δ bands. In the base status, heart-brain coupling primarily depended on the δ band, while in the LA status, β and θ bands dominated in heart-brain coupling. Notably, Candia-Rivera found that θ oscillations occurred during emotion elicitation, indicating that the θ band is actively modulated by vagal inputs under emotion elicitation [43]. The δ band, although less studied in relation to arousal, has demonstrated potential involvement in emotional processing [44]. The close relationship between the θ and δ bands during emotional processing has also been previously described [45]. Various brain regions, including the prefrontal, frontocentral, and parietooccipital regions, have been implicated in the interaction between the brain and the heart during emotion processing [1]. In Fig. 5 (b), midline frontal θ is associated with higher heat-brain coupling in HA status, consistent with Aftanas's report that changes in θ are related to the perceived level of arousal [46]. Aligning with previous studies [13], [47], significant differences in BHI during the processing of positive and negative emotional stimuli are linked to EEG oscillations in the θ band. Furthermore, BHI appears associated with arousal elicitation, with a preference for EEG oscillations in the θ band, especially over the temporal and occipital cortices. While lateralization of brain regions has been proposed as part of differential emotional processing [19], major differences in arousal between the left and right hemispheres were not observed in our study. It is speculated that these differences may arise due to variations in elicitation media (images vs. video) or the diverse valence/arousal levels implemented in the two experimental setups.

C. Limitations and Future Directions

Our study acknowledges several limitations warranting attention. One notable constraint is the lack of integration with clinical laboratory results, hindering the exploration of relationships between coupled heart-brain network features and relevant biomarkers. Incorporating clinical laboratory data is crucial to unveil neurooscillator-based biomarkers, shedding light on the neurobiological underpinnings of emotional processes. Future research should prioritize integrating clinical laboratory data to establish robust connections between heart-brain dynamics and specific biochemical markers associated with distinct emotional states. Additionally, the temporal scope of our data presents a limitation. Extending data collection duration is essential to elucidate dynamic changes in heart-brain coupling across various emotion generation stages. A

more extensive investigation would yield a comprehensive understanding of temporal evolution and variability in dynamic functional connections during emotional processing. Furthermore, while our study employs TDS to quantify coupling strength between mind and brain, it is essential to acknowledge the method's inherent limitations. TDS primarily assesses coupling strength without addressing the directional aspects of these connections. To overcome this limitation, future research could refine or complement TDS with methodologies such as Granger causality analysis or maximum information coefficient, enhancing understanding of directional mind-brain coupling during emotional processing. This multifaceted analytical approach would advance our understanding of the complex interplay between cognitive and emotional mechanisms.

V. CONCLUSION

In summary, our study employs a network physiology methodology, utilizing TDS as a quantifying measure for the coupling strength between the brain and heart in response to visual emotional elicitation. We emphasize the potential role of low-frequency components, specifically in the δ, θ, and α bands of the EEG, in facilitating information transmission during the focused processing of emotion-related stimuli by the brain. Exploring intra-channel interactions among brain rhythms across different emotional states reveals distinct patterns. Surrogate analysis demonstrates the greater reliability of the TDS method in identifying physiological coupling compared to traditional cross-correlation analyses. Notably, the frontal regions, particularly in the context of δ-θ coupling, BHI emerges as pivotal in emotional mediation compared to the central and occipital regions. Surprisingly, our findings indicate no significant difference in BHI between the left and right hemispheres during emotion processing. However, a preference for EEG oscillations, particularly in the θ band, is evident over the prefrontal cortex. This study provides novel insights into the synchronous dynamics between cortical and heartbeat activities during emotional elicitation, highlighting the necessity for nonlinear analysis approaches to comprehensively characterize functional BHI.

REFERENCES AND FOOTNOTES

[1] S. Mishra, N. Srinivasan, and U. S. Tiwary, "Cardiac–Brain Dynamics Depend on Context Familiarity and Their Interaction Predicts Experience of Emotional Arousal," *Brain Sciences*, vol. 12, no. 6, p. 702, May 2022.

[2] M. Wu, W. Teng, C. Fan, S. Pei, P. Li, and Z. Lv, "An Investigation of Olfactory-Enhanced Video on EEG-Based Emotion Recognition," *IEEE Transactions on Neural Systems and Rehabilitation Engineering*, vol. 31, pp. 1602–1613, 2023.

[3] O. Komarov, L.-W. Ko, and T.-P. Jung, "Associations Among Emotional State, Sleep Quality, and Resting-State EEG Spectra: A Longitudinal Study in Graduate Students," *IEEE Transactions on Neural Systems and Rehabilitation Engineering*, vol. 28, no. 4, pp. 795–804, Apr. 2020.

[4] A. Tandle, N. Jog, A. Dharmadhikari, and S. Jaiswal, "Estimation of valence of emotion from musically stimulated EEG using frontal theta asymmetry," in *2016 12th International Conference on Natural Computation, Fuzzy Systems and Knowledge Discovery (ICNC-FSKD)*. Changsha, China: IEEE, Aug. 2016, pp. 63–68.

[5] A. Uusberg, R. Thiruchselvam, and J. J. Gross, "Using distraction to regulate emotion: Insights from EEG theta dynamics," *International Journal of Psychophysiology*, vol. 91, no. 3, pp. 254–260, Mar. 2014.

[6] P. Gao, Z. Long, Z. Xiao, F. Yang, J. Zhang, and G. Liu, "Effects of Acute Moderate Intensity Exercise on Emotion Based on beta Power in EEG," in *Proceedings of the 2019 3rd International Conference on Computer Science and Artificial Intelligence*. Normal IL USA: ACM, Dec. 2019, pp. 283–288.

[7] M. Tortella-Feliu, A. Morillas-Romero, M. Balle, J. Llabrés, X. Bornas, and P. Putman, "Spontaneous EEG activity and spontaneous emotion regulation," *International Journal of Psychophysiology*, vol. 94, no. 3, pp. 365–372, Dec. 2014.

[8] K. Yang, L. Tong, J. Shu, N. Zhuang, B. Yan, and Y. Zeng, "High Gamma Band EEG Closely Related to Emotion: Evidence From Functional Network," *Frontiers in Human Neuroscience*, vol. 14, p. 89, Mar. 2020.

[9] Y. Peng, F. Jin, W. Kong, F. Nie, B.-L. Lu, and A. Cichocki, "OGSSL: A Semi-Supervised Classification Model Coupled With Optimal Graph Learning for EEG Emotion Recognition," *IEEE Transactions on Neural Systems and Rehabilitation Engineering*, vol. 30, pp. 1288–1297, 2022.

[10] W.-L. Zheng, J.-Y. Zhu, and B.-L. Lu, "Identifying Stable Patterns over Time for Emotion Recognition from EEG," *IEEE Transactions on Affective Computing*, vol. 10, no. 3, pp. 417–429, Jul. 2019.

[11] K. Tao, Y. Huang, Y. Shen, and L. Sun, "Automated Stress Recognition Using Supervised Learning Classifiers by Interactive Virtual Reality Scenes," *IEEE Transactions on Neural Systems and Rehabilitation Engineering*, vol. 30, pp. 2060–2066, 2022.

[12] B. K. Steiger, L. C. Kegel, E. Spirig, and H. Jokeit, "Dynamics and diversity of heart rate responses to a disaster motion picture," *International Journal of Psychophysiology*, vol. 143, pp. 64–79, Sep. 2019.

[13] G. Valenza, A. Greco, A. Gentili, A. Lanata, L. Sebastiani, D. Menicucci, A. Gemignani, and E. P. Scilingo, "Combining electroencephalographic activity and instantaneous heart rate for assessing brain–heart dynamics during visual emotional elicitation in healthy subjects," *Philosophical Transactions of the Royal Society A: Mathematical, Physical and Engineering Sciences*, vol. 374, no. 2067, p. 20150176, May 2016.

[14] L. Semeia, I. Bauer, K. Sippel, J. Hartkopf, N. K. Schaal, and H. Preissl, "Impact of maternal emotional state during pregnancy on fetal heart rate variability," *Comprehensive Psychoneuroendocrinology*, vol. 14, p. 100181, May 2023.

[15] M. Mather and J. F. Thayer, "How heart rate variability affects emotion regulation brain networks," *Current Opinion in Behavioral Sciences*, vol. 19, pp. 98–104, Feb. 2018.

[16] Y. Wu, R. Gu, Q. Yang, and Y.-j. Luo, "How Do Amusement, Anger and Fear Influence Heart Rate and Heart Rate Variability?" *Frontiers in Neuroscience*, vol. 13, p. 1131, Oct. 2019.

[17] N. Sabor, H. Mohammed, Z. Li, and G. Wang, "BHI-Net: Brain-Heart Interaction-Based Deep Architectures for Epileptic Seizures and Firing Location Detection," *IEEE Transactions on Neural Systems and Rehabilitation Engineering*, vol. 30, pp. 1576–1588, 2022.

[18] E. Patron, R. Mennella, S. Messerotti Benvenuti, and J. F. Thayer, "The frontal cortex is a heart-brake: Reduction in delta oscillations is associated with heart rate deceleration," *NeuroImage*, vol. 188, pp. 403–410, Mar. 2019.

[19] A. Greco, L. Faes, V. Catrambone, R. Barbieri, E. P. Scilingo, and G. Valenza, "Lateralization of directional brain-heart information transfer during visual emotional elicitation," *American Journal of Physiology-Regulatory, Integrative and Comparative Physiology*, vol. 317, no. 1, pp. R25–R38, Jul. 2019.

[20] P. Taggart, M. R. Boyett, S. Logantha, and P. D. Lambiase, "Anger, Emotion, and Arrhythmias: From Brain to Heart," *Frontiers in Physiology*, vol. 2, 2011.

[21] D. Sammler, M. Grigutsch, T. Fritz, and S. Koelsch, "Music and emotion: Electrophysiological correlates of the processing of pleasant and unpleasant music," *Psychophysiology*, vol. 44, no. 2, pp. 293–304, Mar. 2007.

[22] M. Balconi, E. Grippa, and M. E. Vanutelli, "What hemodynamic (fNIRS), electrophysiological (EEG) and autonomic integrated measures can tell us about emotional processing," *Brain and Cognition*, vol. 95, pp. 67–76, Apr. 2015.

[23] Y.-Y. Tang, Y. Ma, Y. Fan, H. Feng, J. Wang, S. Feng, Q. Lu, B. Hu, Y. Lin, J. Li, Y. Zhang, Y. Wang, L. Zhou, and M. Fan, "Central and autonomic nervous system interaction is altered by short-term meditation," *Proceedings of the National Academy of Sciences*, vol. 106, no. 22, pp. 8865–8870, Jun. 2009.

[24] V. Catrambone, A. Greco, N. Vanello, E. P. Scilingo, and G. Valenza, "Time-Resolved Directional Brain–Heart Interplay Measurement Through Synthetic Data Generation Models," *Annals of Biomedical Engineering*, vol. 47, no. 6, pp. 1479–1489, Jun. 2019.

[25] K. Schiecke, A. Schumann, F. Benninger, M. Feucht, K.-J. Baer, and P. Schlattmann, "Brain–heart interactions considering complex physiological data: Processing schemes for time-variant, frequency-dependent, topographical and statistical examination of directed interactions by convergent cross mapping," *Physiological Measurement*, vol. 40, no. 11, p. 114001, Nov. 2019.

[26] G. M. Dimitri, E. Beqiri, M. M. Placek, M. Czosnyka, N. Stocchetti, A. Ercole, P. Smielewski, P. Lió, the CENTER-TBI Collaborators, A. Anke, R. Beer, B.-M. Bellander, E. Beqiri, A. Buki, M. Cabeleira, M. Carbonara, A. Chieregato, G. Citerio, H. Clusmann, E. Czeiter, M. Czosnyka, B. Depreitere, A. Ercole, S. Frisvold, R. Helbok, S. Jankowski, D. Kondziella, L.-O. Koskinen, A. Kowark, D. K. Menon, G. Meyfroidt, K. Moeller, D. Nelson, A. Piippo-Karjalainen, A. Radoi, A. Ragauskas, R. Raj, J. Rhodes, S. Rocka, R. Rossaint, J. Sahuquillo, O. Sakowitz, P. Smielewski, N. Stocchetti, N. Sundström, R. Takala, T. Tamosuitis, O. Tenovuo, A. Unterberg, P. Vajkoczy, A. Vargiolu, R. Vilcinis, S. Wolf, A. Younsi, and F. A. Zeiler, "Modeling Brain–Heart Crosstalk Information in Patients with Traumatic Brain Injury," *Neurocritical Care*, vol. 36, no. 3, pp. 738–750, Jun. 2022.

[27] A. Bashan, R. P. Bartsch, Jan. W. Kantelhardt, S. Havlin, and P. C. Ivanov, "Network physiology reveals relations between network topology and physiological function," *Nature Communications*, vol. 3, no. 1, p. 702, Feb. 2012.

[28] H. Abdalbari, M. Durrani, S. Pancholi, N. Patel, S. J. Nasuto, and N. Nicolaou, "Brain and brain-heart Granger causality during wakefulness and sleep," *Frontiers in Neuroscience*, vol. 16, p. 927111, Sep. 2022.

[29] L. Faes, D. Marinazzo, F. Jurysta, and G. Nollo, "Linear and non-linear brain–heart and brain–brain interactions during sleep," *Physiological Measurement*, vol. 36, no. 4, pp. 683–698, Apr. 2015.

[30] K. Schiecke, B. Pester, D. Piper, F. Benninger, M. Feucht, L. Leistritz, and H. Witte, "Nonlinear Directed Interactions Between HRV and EEG Activity in Children With TLE," *IEEE Transactions on Biomedical Engineering*, vol. 63, no. 12, pp. 2497–2504, Dec. 2016.

[31] R. Agarwal, M. Andujar, and S. Canavan, "Classification of emotions using EEG activity associated with different areas of the brain," *Pattern Recognition Letters*, vol. 162, pp. 71–80, Oct. 2022.

[32] A. Roshdy, S. Alkork, A. S. Karar, H. Mhalla, T. Beyrouthy, Z. Al Barakeh, and A. Nait-ali, "Statistical Analysis of Multi-channel EEG Signals for Digitizing Human Emotions," in *2021 4th International Conference on Bio-Engineering for Smart Technologies (BioSMART)*. Paris / Créteil, France: IEEE, Dec. 2021, pp. 1–4.

[33] V. Kalidas and L. Tamil, "Real-time QRS detector using Stationary Wavelet Transform for Automated ECG Analysis," in *2017 IEEE 17th International Conference on Bioinformatics and Bioengineering (BIBE)*. Washington, DC: IEEE, Oct. 2017, pp. 457–461.

[34] K. A. Lindquist, A. B. Satpute, T. D. Wager, J. Weber, and L. F. Barrett, "The Brain Basis of Positive and Negative Affect: Evidence from a Meta-Analysis of the Human Neuroimaging Literature," *Cerebral Cortex*, vol. 26, no. 5, pp. 1910–1922, May 2016.

[35] D. Schubring and H. T. Schupp, "Emotion and Brain Oscillations: High Arousal is Associated with Decreases in Alpha- and Lower Beta-Band Power," *Cerebral Cortex*, vol. 31, no. 3, pp. 1597–1608, Feb. 2021.

[36] K. M. Hartikainen, "Emotion-Attention Interaction in the Right Hemisphere," *Brain Sciences*, vol. 11, no. 8, p. 1006, Jul. 2021.

[37] G. Zhao, Y. Zhang, and Y. Ge, "Frontal EEG Asymmetry and Middle Line Power Difference in Discrete Emotions," *Frontiers in Behavioral Neuroscience*, vol. 12, p. 225, Nov. 2018.

[38] D. Sander, D. Grandjean, G. Pourtois, S. Schwartz, M. L. Seghier, K. R. Scherer, and P. Vuilleumier, "Emotion and attention interactions in social cognition: Brain regions involved in processing anger prosody," *NeuroImage*, vol. 28, no. 4, pp. 848–858, Dec. 2005.

[39] N. E. Adams, C. Teige, G. Mollo, T. Karapanagiotidis, P. L. Cornelissen, J. Smallwood, R. D. Traub, E. Jefferies, and M. A. Whittington, "Theta/delta coupling across cortical laminae contributes to semantic cognition," *Journal of Neurophysiology*, vol. 121, no. 4, pp. 1150–1161, Apr. 2019.

[40] T. Stankovski, V. Ticcinelli, P. V. E. McClintock, and A. Stefanovska, "Neural Cross-Frequency Coupling Functions," *Frontiers in Systems Neuroscience*, vol. 11, p. 33, Jun. 2017.

[41] D. J. L. G. Schutter and G. G. Knyazev, "Cross-frequency coupling of brain oscillations in studying motivation and emotion," *Motivation and Emotion*, vol. 36, no. 1, pp. 46–54, Mar. 2012.

[42] S. Garcia-Retortillo, C. Romero-Gómez, and P. C. Ivanov, "Network of muscle fibers activation facilitates inter-muscular coordination, adapts to fatigue and reflects muscle function," *Communications Biology*, vol. 6, no. 1, p. 891, Aug. 2023.

[43] D. Candia-Rivera, V. Catrambone, J. F. Thayer, C. Gentili, and G. Valenza, "Cardiac sympathetic-vagal activity initiates a functional brain–body response to emotional arousal," *Proceedings of the National Academy of Sciences*, vol. 119, no. 21, p. e2119599119, May 2022.

[44] M. A. Klados, C. Frantzidis, A. B. Vivas, C. Papadelis, C. Lithari, C. Pappas, and P. D. Bamidis, "A Framework Combining Delta Event-Related Oscillations (EROs) and Synchronisation Effects (ERD/ERS) to Study Emotional Processing," *Computational Intelligence and Neuroscience*, vol. 2009, pp. 1–16, 2009.

[45] G. Knyazev, J. Slobodskoj-Plusnin, and A. Bocharov, "Event-related delta and theta synchronization during explicit and implicit emotion processing," *Neuroscience*, vol. 164, no. 4, pp. 1588–1600, Dec. 2009.

[46] L. I. Aftanas and S. A. Golocheikine, "Human anterior and frontal midline theta and lower alpha re¯ect emotionally positive state and internalized attention: High-resolution EEG investigation of meditation," *Neuroscience Letters*, 2001.

[47] M. Y. Bekkedal, J. Rossi, and J. Panksepp, "Human brain EEG indices of emotions: Delineating responses to affective vocalizations by measuring frontal theta event-related synchronization," *Neuroscience & Biobehavioral Reviews*, vol. 35, no. 9, pp. 1959–1970, Oct. 2011.